

reaction was monitored by GC. After considerable consumption (60–99%) of the starting enone (approximately 28–50 h) the solvent was removed by distillation under reduced pressure. Chromatographic purification (silica gel, 200 mesh) of the reaction mixture eluting with petroleum ether/ethyl acetate gave the cyclization product (**3a–d**, **5**, or **8**) along with Ph_3PO . DCA was recovered (98%). The products were characterized by ^1H and ^{13}C NMR spectroscopy and mass spectrometry. **3a** and **3b** were confirmed by comparing with authentic samples [9].

Received: August 18, 1993

Revised version: January 26, 1994 [Z 6292 IE]

German version: *Angew. Chem.* **1994**, *106*, 1217

- [1] Selected reviews: I. Willner, B. Willner, *Top. Curr. Chem.* **1991**, *159*, 157, and references therein; S. E. Webber, *Chem. Rev.* **1990**, *90*, 1469; T. J. Meyer, *Coord. Chem. Rev.* **1991**, *111*, 47; M. A. Fox, *Adv. Photochem.* **1986**, *13*, 237.
- [2] M. A. Fox, M. Chanon, *Photoinduced Electron Transfer Reactions*, Part D, Elsevier, Amsterdam, **1988**; P. S. Mariano, J. L. Stavinoha, *Synthetic Organic Photochemistry* (Ed.: W. M. Horspool), Plenum Press, New York, **1984**, p. 145; S. L. Mattes, S. Farid, *Org. Photochem.* **1983**, *6*, 223.
- [3] G. Pandey, *Top. Curr. Chem.* **1993**, *168*, 175; J. Mattay, *Synthesis* **1989**, 233.
- [4] T. Hamada, A. Nishida, O. Yonemitsu, *J. Am. Chem. Soc.* **1986**, *108*, 140; K. Okada, K. Okamoto, M. Oka, *ibid.* **1988**, *110*, 8736. However, the mechanism of the regeneration of the light-absorbing electron donor is not yet known.
- [5] G. Pandey, *Synlett* **1992**, 546; G. Pandey, B. B. V. Soma Sekhar, U. T. Bhalerao, *J. Am. Chem. Soc.* **1990**, *112*, 5650; G. Pandey, B. B. V. Soma Sekhar, *J. Org. Chem.* **1992**, *57*, 4019.
- [6] G. Pandey, D. Pooranchand, U. T. Bhalerao, *Tetrahedron* **1991**, *47*, 1745; D. Pooranchand, Dissertation, Osmania University, **1992**.
- [7] The only analogy to this concept may be found in artificial photosynthesis [1] and glutathione reduction (I. Willner, N. Lapidot, *J. Am. Chem. Soc.* **1991**, *113*, 3625.)
- [8] T. Majima, C. Pac, A. Nakasone, H. Sakurai, *J. Am. Chem. Soc.* **1981**, *103*, 4499.
- [9] E. J. Enholm, K. S. Kinter, *J. Am. Chem. Soc.* **1991**, *113*, 7784.
- [10] Bioanalytical systems, model CV-27; Pt inlay working electrode, Ag/AgCl reference electrode, and Pt wire auxiliary electrode; tetraethyl ammonium perchlorate in DMF as the supporting electrolyte. The DMF solution was degassed by argon bubbling for 10 minutes before each measurement.
- [11] Since the reduction potentials are irreversible, the ΔG_{ET} values obtained are only approximate; however, they agree generally quite well with experimental values.
- [12] DMF was used as solvent mainly because of the higher solubility of DCA. The reaction can also be performed in acetonitrile, but reaction times are longer owing to the poor solubility of DCA.
- [13] Control experiments in the dark or with irradiation (405 nm) but without Ph_3P give no reaction product.
- [14] J. Mattay, A. Banning, E. W. Bischof, A. Heidbreder, J. Runsink, *Chem. Ber.* **1992**, *125*, 2119.
- [15] J. G. Calvert, J. N. Pitts, *Photochemistry*, Wiley, New York, **1966**, p. 736.

N-Heteroarene Dianions as Antiaromatic Ligands Bridging two Lanthanocene Moieties**

Joachim Scholz,* Annett Scholz, Roman Weimann, Christoph Janiak, and Herbert Schumann

Pyrazine serves as a model ligand for studying magnetic exchange phenomena,^[1] electron transfer reactions,^[2] or one-dimensional conductors.^[3] With its two N-donor functions, this heterocycle can coordinate to Lewis acidic metal centers and at the same time bridge two metal atoms.^[4] The π -acceptor characteristics (low-lying LUMOs) of this bridging ligand enable, un-

[*] Dr. J. Scholz, Dipl.-Chem. A. Scholz
Institut für Anorganische Chemie der Universität Halle-Wittenberg
Geusaer Strasse, D-06217 Merseburg (FRG)
Telefax: Int. code + (3461)46-2370

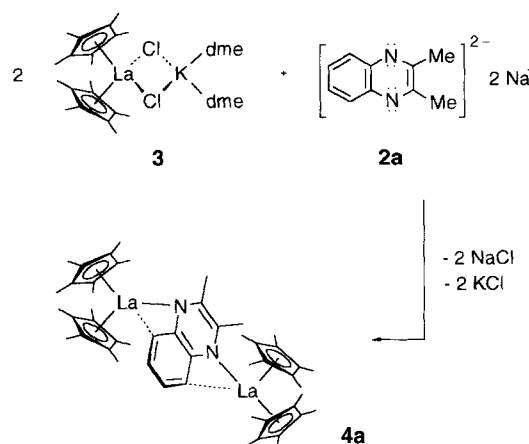
Prof. Dr. H. Schumann, Dr. R. Weimann, Dr. C. Janiak
Institut für Anorganische und Analytische Chemie
der Technischen Universität Berlin (FRG)

[**] This work was supported by the Fonds der Chemischen Industrie. We thank Prof. Dr. K.-H. Thiele for his interest.

der suitable conditions, the generation of, for example, stable radical ions from these binuclear complexes.^[5]

Quinoxaline and phenazine represent benzo- and dibenzo-annulated derivatives of pyrazine, respectively; in contrast to the parent compound pyrazine, these heterocycles can be reduced to their dianions either electrochemically^[6] or by alkali metals.^[7] The formally antiaromatic systems with 12- π and 16- π electrons have high charge density and, so far, could be stabilized in only a few cases by presence of alkali and alkaline earth ions.^[8] We have found now that the resulting electron-rich N-heteroarene dianions can bridge two lanthanocene moieties. Here we report on the synthesis and crystal structure analysis of complexes **4a** and **4b**, which are the first examples of this new class of compounds.

2,3-Dimethylquinoxaline (**1a**) is rapidly reduced by two equivalents of sodium in THF to give a deep blue solution containing the 12- π dianion **2a**. This dianion reacts with **3** in a 2:1 molar ratio to yield the novel, binuclear lanthanocene complex **4a**, which can be isolated as dark green, extremely air- and moisture-sensitive crystals (Scheme 1). On the basis of the NMR



Scheme 1. dme = dimethoxyethane.

spectra one can already expect unusual bonding properties for this compound. For example, the signals for H atoms H24 and H24a' ($\delta = 4.22$) and for H25 and H25a' ($\delta = 5.66$, AA'XX' spin system, numbering scheme according to Fig. 1) of the 2,3-dimethylquinoxaline heterocycle are shifted to higher field by $\Delta\delta = 3$ and 2.4, respectively, when compared to the free ligand.^[9] The nonuniform charge distribution is indicative of a paramagnetic ring current, which is characteristic for systems with $4n\pi$ electrons such as naphthalene-lithium $\text{Li}_2[\text{C}_{10}\text{H}_8]$.^[10b] Atoms C24 and C24' of the bridging ligand are also strongly shielded ($\delta = 89.9$). In contrast to the ^1H NMR signals, the ^{13}C NMR signal positions are barely influenced by ring-current effects and reflect, for the most part, the actual charge distribution. Hence, the negative charge density in the bridging ligand of **4a** is even higher than in 2,3-diphenylquinoxaline disodium $\text{Na}_2[\text{C}_8\text{H}_4\text{N}_2(2,3\text{-Ph}_2)]$ (corresponding signal at $\delta = 100.3$).^[7] This observation contrasts with those for the recently described 1,4-dihydroquinoxaline derivative 1,4- $[\text{Me}_2(\text{tBu})\text{Si}]_2(\text{C}_8\text{H}_6\text{N}_2)$ in which the charge density of the $4n\pi$ electron system is transferred to the stabilizing R_3Si -acceptor substituents through covalent N-Si bonds; moreover, the extent of electron delocalization from the heteroarene to the arene unit is small.^[8c]

Figure 1 shows the result of the X-ray structure analysis of **4a**.^[11] The two Cp^*_2La moieties face each other and are bound

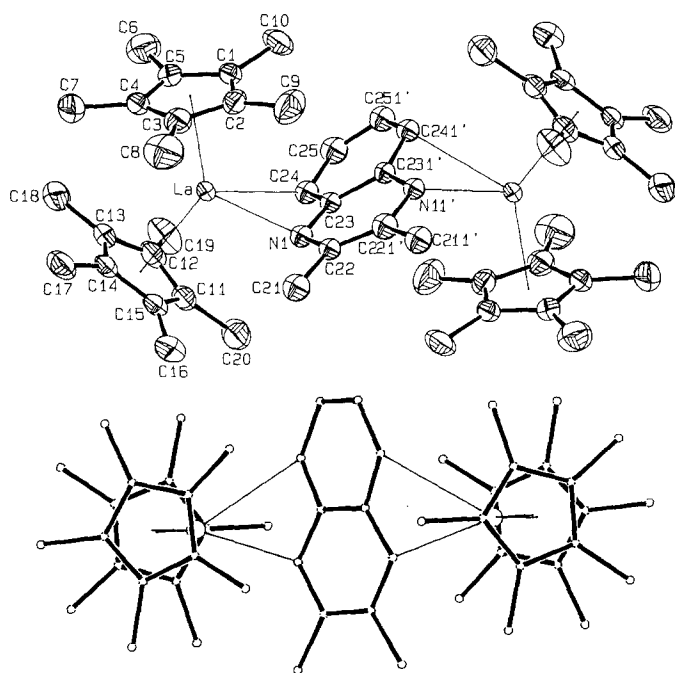


Fig. 1. Structure of **4a** in the crystal. The 2,3-dimethylquinoxaline dianion is disordered and occupies one of two molecular positions. These positions are twisted relative to each other by 180°. For clarity only one of the two arrangements is shown. Top: ORTEP view. Selected bond lengths [Å] and angles [°] (Cp*1 and Cp*2 represent centroid positions of the η^5 -bonded cyclopentadienyl ligands C1–C5 and C11–C15): La–N1 2.409(4), La–N1a 2.444(4), La–Cp*1 2.521(1), La–Cp*2 2.537(1), La–C23 2.846(5), La–C23a 2.918(4), La–C24 2.903(5), La–C24a 2.891(5), N1–C22 1.400(6), N1–C23 1.355(6), N1a–C22a 1.391(6), N1a–C23a 1.360(6), C22–C22a 1.37(1), C23–C23a 1.445(8), C24–C25 1.419(7), C24a–C25a 1.453(7), C23–C24 1.376(7), C23a–C24a 1.400(7), C25–C25a 1.37(1), Cp*1–La–Cp*2 136.6(1). Bottom: The complex viewed from above to clarify the bonding.

to the planar quinoxaline dianion. From an electrostatic point of view the N atoms of the bridging ligand are the more favorable ligating atoms for the lanthanocene moieties; hence, the La–N contacts are short [La–N1 2.409(4), La–N1a 2.444(4) Å] and are of the same magnitude as La–N distances reported previously.^[12] The two La atoms are located 1.770(5) Å below and above the quinoxaline plane. This finding is indicative of a partial π character for the La–N interactions. Additional interactions with quinoxaline atoms C24 and C24' are in line with the tendency of La atoms to attain a higher coordination number. The La–C distances are only marginally larger than the average La–C_{Cp*} distance (2.789 and 2.806 Å) or those reported recently for the [La(η^3 -C₃H₅)₄][–] ion (La–C_{average} 2.811 Å).^[13] The remarkable high-field positions of the ¹³C NMR signals of C24 and C24' and the relatively small ¹J_{C,H} coupling constant of only 144.4 Hz indicate that these La–C interactions persist even in solution and that an agostic C–H→La bond is present.

The ¹H NMR spectrum of the phenazine complex **4b** points to a similar bonding arrangement. This complex is obtained in form of orange crystals when a bordeaux-red suspension of Na₂[C₁₂H₈N₂] (**2b**, prepared by reacting phenazine (**1b**) with Na granules in THF for several days) is added to **3**. Complex **4b** is extremely air- and moisture-sensitive and is less soluble in *n*-pentane, diethyl ether, or toluene than **4a**. Figure 2 shows the structure of **4b** in the crystal.^[11] The important structural characteristics of **4a** and **4b** are

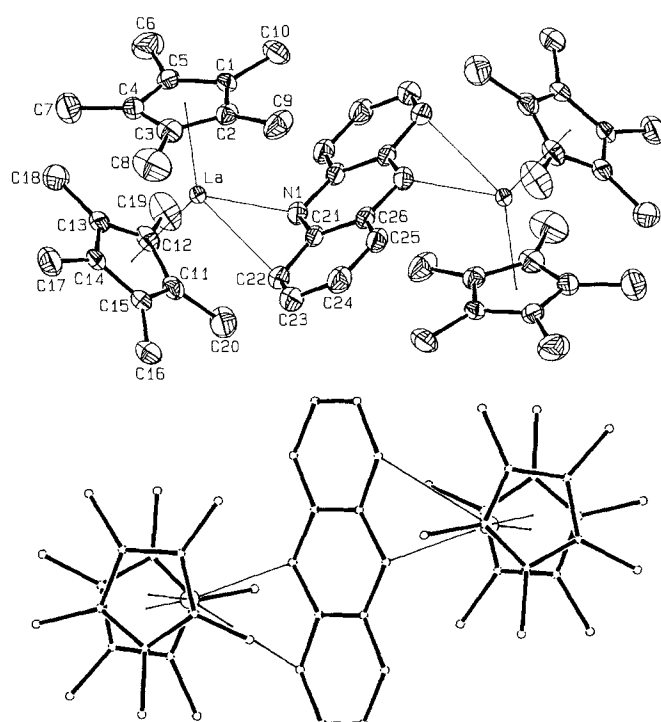
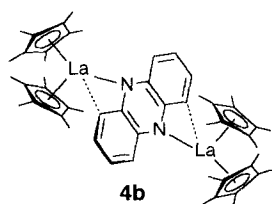


Fig. 2. Structure of **4b** in the crystal. Top: ORTEP view. Selected bond lengths [Å] and angles [°] (Cp*1 and Cp*2 represent the centroid positions of the η^5 -bonded cyclopentadienyl ligands C1–C5 and C11–C15): La–N1 2.452(2), La–C21 2.920(2), La–C22 2.931(2), La–Cp*1 2.525(1), La–Cp*2 2.541(1), N1–C21 1.383(3), C21–C22 1.403(3), C22–C23 1.401(4), C23–C24 1.368(4), C24–C25 1.404(4), C25–C26 1.389(3), C21–C26 1.427(3), Cp*1–La–Cp*2 135.9(1). Bottom: The complex as viewed from above in order to clarify the bonding.

identical. As in **4a**, the La atoms in **4b** are bound to the planar bridging ligand by short contacts with the N atoms and by additional interactions with C22 and C22'. The La atoms are positioned 1.870(5) Å above and below the phenazine plane. The outstanding structural feature of **4b** is, without a doubt, the staggered arrangement of the two Cp*₂La moieties on the periphery of the bridging ligand. In this arrangement the dipolar repulsion between the two Cp*₂La moieties is minimized.

The bonding interaction between the La atoms and the carbon atoms of the bridging ligands (i.e., C24 and C24' in **4a**, C22 and C22' in **4b**) can easily be rationalized. A PM3 calculation^[14] for the phenazine- and the 2,3-dimethylquinoxaline dianion shows not only the expected high charge density on the N atoms but also charge maxima located at exactly those ring carbon atoms (Fig. 3). In contrast, quaternary C atoms (i.e., C23 and C23' in **4a**, C21 and C21' in **4b**) adjacent to the N atoms are positively polarized. Their relatively short distance to the La atoms is, therefore, not the result of a bonding interaction with the metal but is apparently forced by the special manner of coordination behavior of the bridging ligands. Relative and absolute bond length variations of the N heterocycles,^[9] as determined by crystal structure analysis of **4a** and **4b**, can also be rationalized by PM3 optimization of their respective dianionic structures.

Even in unpolar solvents such as [D₈]toluene, the partial La–N π interaction, which explains the deflection of the Cp*₂La moieties out of the heteroarene plane, is apparently removed. All four Cp* ligands of **4a** and **4b** show only one sharp signal in the ¹H NMR spectrum at room temperature. This Cp* signal, as well as the signals for the H atoms of the 2,3-dimethylquinoxaline in **4a** remain almost unchanged upon cooling the sample

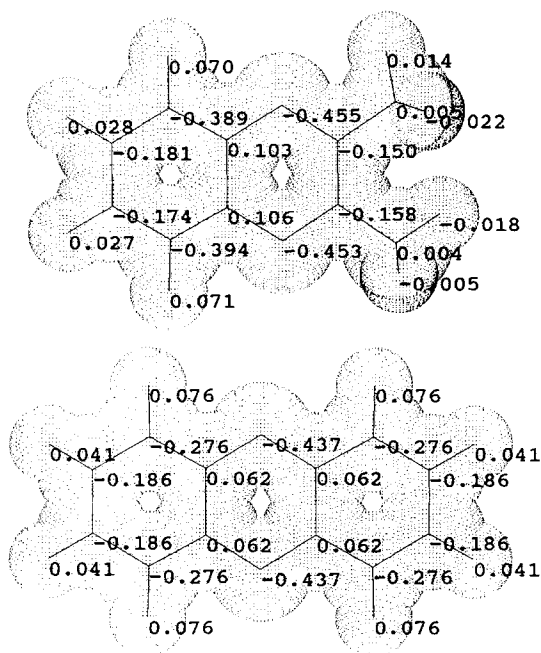


Fig. 3. Charge distribution for the PM3-optimized [14] 2,3-dimethylquinoxaline (top) and phenazine dianions (bottom).

to -80°C (500 MHz; see Experimental Procedure). However, it cannot be ruled out that even at low temperatures the Cp^*_2La moieties, for example, rotate around the $\text{La}-\text{N}$ bond. It is worth mentioning that cooling of a toluene solution of **4a** results in a reversible color change from green to dark red.

Complexes **4a** and **4b** represent a novel structural type for organolanthanides, which is reminiscent of the mostly ionic "aromatic alkali-metal amides"^[15] Due to their high charge density both the quinoxaline and the phenazine dianions, which can be regarded as heteroatom-modified $4n\pi$ anti-Hückel systems, are of special interest as "molecular bridges". We are currently investigating complexes in which two paramagnetic metal centers are connected by these antiaromatic bridging ligands.

Experimental Procedure

All experiments were carried out with thoroughly dried and degassed solvents under an inert argon atmosphere.

4a: In 100 mL THF 2,3-dimethylquinoxaline (1.29 g, 8.15 mmol) was treated with sodium (0.375 g, 16.31 mmol), until all of the metal had been consumed and a deep blue solution was formed. This solution was then added dropwise at -50°C to a solution of $[\text{Cp}^*_2\text{La}(\mu\text{-Cl})_2\text{K}(\text{dme})_2]$, prepared by adding LaCl_3 (4.0 g, 16.31 mmol) to $[\text{Cp}^*\text{K}(\text{dme})_2]$ (8.61 g, 32.6 mmol) in 200 mL THF. After warming the reaction mixture to room temperature and removing the solvent under vacuum, **4a** was isolated by extraction of the residue with 100 mL diethyl ether. Recrystallization from *n*-pentane yielded 2.77 g (17%) of dark green crystals, which were suitable for crystal structure analysis. $T_{\text{decomp.}} \approx 115^{\circ}\text{C}$. Correct elemental analysis.— ^1H NMR (300 MHz, C_6D_6 , 20°C): $\delta = 5.66$ (m, $^3J(\text{H}_A, \text{H}_X) = 6.0$ Hz, $^4J(\text{H}_A, \text{H}_X) = 1.3$ Hz, 2H; $\text{C}_8\text{H}_4\text{N}_2\text{-2,3-Me}_2$), 4.22 (m, $^3J(\text{H}_A, \text{H}_X) = 6.0$ Hz, $^4J(\text{H}_A, \text{H}_X) = 1.3$ Hz, 2H; $\text{C}_8\text{H}_4\text{N}_2\text{-2,3-Me}_2$), 2.22 (s, 60H; C_5Me_5), 1.50 (s, 6H; $\text{C}_8\text{H}_4\text{N}_2\text{-2,3-Me}_2$); ^1H NMR (500 MHz, $[\text{D}_8]\text{toluene}$, -80°C): $\delta = 5.73$ (m, 2H; $\text{C}_8\text{H}_4\text{N}_2\text{-2,3-Me}_2$), 4.23 (m, 2H; $\text{C}_8\text{H}_4\text{N}_2\text{-2,3-Me}_2$), 2.04 (s, 60H; C_5Me_5), 1.50 (s, 6H; $\text{C}_8\text{H}_4\text{N}_2\text{-2,3-Me}_2$); ^{13}C NMR (75 MHz, C_6D_6 , 25°C): $\delta = 150.7$ (s, $\text{C}_8\text{H}_4\text{N}_2\text{-2,3-Me}_2$), 122.2 (s, $\text{C}_8\text{H}_4\text{N}_2\text{-2,3-Me}_2$), 119.8 (dd, $^1J(\text{C,H}) = 159.3$ Hz; $\text{C}_8\text{H}_4\text{N}_2\text{-2,3-Me}_2$), 119.1 (s, C_5Me_5), 89.9 (ddd, $^1J(\text{C,H}) = 144.4$ Hz; $\text{C}_8\text{H}_4\text{N}_2\text{-2,3-Me}_2$), 18.5 (q, $^1J(\text{C,H}) = 124.6$ Hz; $\text{C}_8\text{H}_4\text{N}_2\text{-2,3-Me}_2$), 9.6 (q, $^1J(\text{C,H}) = 125.2$ Hz; C_5Me_5).

4b: In 100 mL THF, phenazine (1.47 g, 8.15 mmol) was treated with sodium (0.375 g, 16.31 mmol). The resulting bordeaux-red suspension was then added dropwise at -50°C to a solution of $[\text{Cp}^*_2\text{La}(\mu\text{-Cl})_2\text{K}(\text{dme})_2]$, prepared by adding LaCl_3 (4.0 g, 16.31 mmol) to $[\text{Cp}^*\text{K}(\text{dme})_2]$ (8.61 g, 32.6 mmol) in 200 mL THF. After warming the reaction mixture to room temperature and removing the solvent under vacuum, the residue was extracted with diethyl ether. From this extract, **4b** separated in the form of orange-red crystals (yield 1.63 g, 10%). Recrystallization

of this material from diethyl ether gave single crystals suitable for crystal structure analysis. $T_{\text{decomp.}} \approx 80^{\circ}\text{C}$. Correct elemental analysis.— ^1H NMR (300 MHz, C_6D_6 , 20°C): $\delta = 6.19$ (m, AA'XX', 4H; $\text{C}_{12}\text{H}_8\text{N}_2$), 5.29 (m, AA'XX', 4H; $\text{C}_{12}\text{H}_8\text{N}_2$), 2.06 (s, 60H; C_5Me_5); ^{13}C NMR (75 MHz, C_6D_6 , 25°C): $\delta = 145.5$ ($\text{C}_{12}\text{H}_8\text{N}_2$), 121.1 (C_5Me_5), 119.9, 106.4 ($\text{C}_{12}\text{H}_8\text{N}_2$), 10.6 (C_5Me_5).

Received: December 14, 1993 [Z 65601E]
German version: *Angew. Chem.* **1994**, *106*, 1220

- [1] D. Kahn, *Angew. Chem.* **1985**, *97*, 837–853; *Angew. Chem. Int. Ed. Engl.* **1985**, *24*, 834–850.
- [2] a) W. Kaim, *Angew. Chem.* **1984**, *96*, 609–610; *Angew. Chem. Int. Ed. Engl.* **1984**, *23*, 613–614; b) W. Kaim, *Acc. Chem. Res.* **1985**, *18*, 160–166.
- [3] O. Schneider, M. Hanack, *Angew. Chem.* **1982**, *94*, 68–69; *Angew. Chem. Int. Ed. Engl.* **1982**, *21*, 79–80.
- [4] Numerous examples of such structural variations exist for both main group and transition metals. Of special interest are complexes in which the N heteroarene acts as a π bridging ligand and enables charge transfer between two metal atoms, as is the case in the Creutz–Taube ion $[(\text{NH}_3)_5\text{Ru}(\mu\text{-C}_4\text{H}_4\text{N}_2)_2\text{Ru}(\text{NH}_3)_5]^{3+}$: C. Creutz, H. Taube, *J. Am. Chem. Soc.* **1969**, *91*, 3988–3989; b) *ibid.* **1973**, *95*, 1086–1094; c) U. Fűrholz, H. B. Bürgi, F. E. Wagner, A. Stebler, J. H. Ammeter, E. Krausz, R. J. H. Clark, M. J. Stead, A. Ludi, *ibid.* **1984**, *106*, 121–123; additional examples: d) $(\text{Cp}_2\text{Yb})_2(\mu\text{-C}_4\text{H}_4\text{N}_2)$: E. C. Baker, K. N. Raymond, *Inorg. Chem.* **1977**, *16*, 2710–2714; e) $[(\text{Cp}^*_2\text{Ba})_2(\mu\text{-C}_4\text{H}_4\text{N}_2)]$: R. A. Williams, T. P. Hanusa, J. C. Huffman, *J. Organomet. Chem.* **1992**, *429*, 143–152.
- [5] a) W. Kaim, *Chem. Ber.* **1982**, *115*, 910–918; b) R. Groß, W. Kaim, *Angew. Chem.* **1984**, *96*, 610–611; *Angew. Chem. Int. Ed. Engl.* **1984**, *23*, 614–615; c) R. Groß, W. Kaim, *Inorg. Chem.* **1986**, *25*, 498–506.
- [6] R. M. Crooks, A. J. Bard, *J. Phys. Chem.* **1987**, *91*, 1274–1284.
- [7] A. Minsky, Y. Cohen, M. Rabinovitz, *J. Am. Chem. Soc.* **1985**, *107*, 1501–1505; b) Y. Cohen, A. Y. Meyer, M. Rabinovitz, *ibid.* **1986**, *108*, 7039–7044.
- [8] a) $[\text{Mg}_2\text{Br}_2(\mu\text{-C}_4\text{H}_4\text{N}_2)(\text{thf})_6]$: P. C. Junk, C. L. Raston, B. W. Skelton, A. H. White, *J. Chem. Soc. Chem. Commun.* **1987**, 1162–1164; b) $[\text{Li}_2(\mu\text{-Cl})(\mu\text{-NC}_4\text{H}_4\text{NH})(\text{thf})_4]$: L. M. Engelhardt, G. E. Jacobsen, A. H. White, C. L. Raston, *Inorg. Chem.* **1991**, *30*, 3978–3980; 1,4-dihydropyrazine, 1,4-dihydroquinoxaline, and 1,4-dihydrophenazine compounds that are stabilized by π acceptor substituents (e.g., SiR_3) in the 1,4 position have not been taken into consideration: c) W. Kaim, *Angew. Chem.* **1981**, *93*, 621–622; *Angew. Chem. Int. Ed. Engl.* **1981**, *20*, 600–601; d) 1,4-(Me_3M) $_2\text{C}_4\text{H}_4\text{N}_2$ (M = Si, Ge): H.-D. Hausen, O. Mundt, W. Kaim, *J. Organomet. Chem.* **1985**, *296*, 321–337; e) 1,4-[(*t*Bu)Me $_2$ Si] $_2\text{C}_4\text{H}_4\text{N}_2$: A. Lichtblau, H.-D. Hausen, W. Kaim, *Z. Naturforsch. B* **1993**, *48*, 713–718; f) 1,4-[(*t*Bu)Me $_2$ Si] $_2\text{C}_4\text{Me}_4\text{N}_2$: W. Kaim, A. Lichtblau, H.-D. Hausen, *J. Organomet. Chem.* **1993**, *456*, 167–173.
- [9] **1a:** ^1H NMR (C_6D_6): $\delta = 8.04$ (m, AA'XX', 2H; $\text{C}_8\text{H}_4\text{N}_2\text{-2,3-Me}_2$), 7.21 (m, AA'XX', 2H; $\text{C}_8\text{H}_4\text{N}_2\text{-2,3-Me}_2$), 2.16 (s, 6H; $\text{C}_8\text{H}_4\text{N}_2\text{-2,3-Me}_2$); ^{13}C NMR (C_6D_6): $\delta = 153.5$, 141.9, 128.9, 128.6 ($\text{C}_8\text{H}_4\text{N}_2\text{-2,3-Me}_2$), 22.8 ($\text{C}_8\text{H}_4\text{N}_2\text{-2,3-Me}_2$), **1b:** ^1H NMR (C_6D_6): $\delta = 8.13$ (m, AA'XX', 4H; $\text{C}_{12}\text{H}_8\text{N}_2$), 7.17 (m, AA'XX', 4H; $\text{C}_{12}\text{H}_8\text{N}_2$); ^{13}C NMR (C_6D_6): $\delta = 144.0$, 130.9, 130.3; see also A. E. A. Porter in *Comprehensive Heterocyclic Chemistry*, Vol. 3, Part 2B. (Eds.: A. I. Boulton, A. McKillop), Pergamon Press, Oxford, **1988**, Chap. 2.14; cited references.
- [10] a) $[\text{C}_{16}\text{H}_8]^{2-}$: R. Benken, H. Günther, *Helv. Chim. Acta* **1988**, *71*, 694–702; b) $[\text{C}_{14}\text{H}_6]^{2-}$: K. Müllen, *ibid.* **1976**, *59*, 1357–1359.
- [11] a) Crystal data for **4a**: formula $\text{C}_{50}\text{H}_{70}\text{N}_2\text{La}_2\text{OC}_4\text{H}_{10}$, $M_r = 976.93$ g cm $^{-1}$ (without Et_2O), crystal dimensions $0.30 \times 0.25 \times 0.50$ mm 3 , $a = 1034.8(1)$, $b = 1102.2(2)$, $c = 1148.7(3)$ pm, $\alpha = 81.71(2)$, $\beta = 78.01(2)$, $\gamma = 88.74(1)^\circ$, $V = 1268.2(4) \times 10^6$ pm 3 , $Z = 1$, $\rho_{\text{calc.}} = 1.356$ g cm $^{-3}$, $\mu = 15.82$ cm $^{-1}$, $F(000) = 543$, triclinic crystal system, space group $P\bar{1}$ (No. 2), Enraf–Nonius CAD4 diffractometer, MoK_α radiation, $\lambda = 71.069$ pm, graphite monochromator, temperature 160 K, 4694 measured reflections, 4330 independent ($R_{\text{int}} = 0.0179$) and 4187 observed reflections [$F_o \geq 2\sigma(F_o)$], empirical absorption correction (Ψ scans), 393 parameters refined, $R = 0.021$, $R_w = 0.024$, residual electron density: max. 0.49, min. -0.49 e Å^{-3} . b) **4b**: formula $\text{C}_{52}\text{H}_{68}\text{N}_2\text{La}_2\text{OC}_4\text{H}_{10}$, $M_r = 998.94$ g cm $^{-1}$ (without Et_2O), crystal dimensions $0.30 \times 0.26 \times 0.50$ mm 3 , $a = 1029.0(1)$, $b = 1114.9(2)$, $c = 1142.1(3)$ pm, $\alpha = 82.15(2)$, $\beta = 78.58(2)$, $\gamma = 87.32(1)^\circ$, $V = 1271.9(5) \times 10^6$ pm 3 , $Z = 1$, $\rho_{\text{calc.}} = 1.400$ g cm $^{-3}$, $\mu = 15.72$ cm $^{-1}$, $F(000) = 543$, triclinic crystal system, space group $P\bar{1}$ (No. 2), Enraf–Nonius CAD4 diffractometer, MoK_α radiation, $\lambda = 71.069$ pm, graphite monochromator, temperature 160 K, 4696 measured reflections, 4404 independent ($R_{\text{int}} = 0.0199$) and 4263 observed reflections [$F_o \geq 2\sigma(F_o)$], empirical absorption correction (Ψ scans), 335 parameters refined, $R = 0.019$, $R_w = 0.021$, residual electron density: max. 0.48, min. -0.48 e Å^{-3} . Further details of the crystal structure investigation may be obtained from the Fachinformationszentrum Karlsruhe, D-76344 Eggenstein-Leopoldshafen (FRG), on quoting the depository number CSD-57974 and the journal citation.
- [12] Examples for La–N σ bonds: a) $[(\text{MeC}_2\text{H}_4)_2\text{OCa}(\text{NPh}_2)_2][\text{Li}(\text{dme})_2]$ La–N 2.443(7)–2.469(8) Å, average 2.459(7) Å, J. Guan, S. Jin, Y. Lin, Q. Shen,

- Organometallics* **1992**, *11*, 2483–2847; b) [Cp*₂LaNHCH₃(NH₂CH₃)] La-N 2.323(1) and 2.302(10) Å. La ← N 2.70(1) Å. M. R. Gagné, C. L. Stern, T. J. Marks, *J. Am. Chem. Soc.* **1992**, *114*, 275–294.
- [13] R. Taube, H. Windisch, F. H. Görlitz, H. Schumann, *J. Organomet. Chem.* **1993**, *445*, 85–91.
- [14] J. J. P. Stewart, *J. Comput. Chem.* **1989**, *10*, 209–221; b) J. J. P. Stewart in *Reviews in Computational Chemistry* (Eds.: K. B. Lipkowitz, D. B. Boyd), VCH, Weinheim, **1990**, p. 45 ff.
- [15] a) R. Hacker, E. Kaufmann, P. von Ragué Schleyer, W. Mahdi, H. Dietrich, *Chem. Ber.* **1987**, *120*, 1533–1538; b) K. Gregory, M. Bremer, P. von Ragué Schleyer, P. A. A. Klusener, L. Brandsma, *Angew. Chem.* **1989**, *101*, 1261–1264; *Angew. Chem. Int. Ed. Engl.* **1989**, *28*, 1224–1226.

Catalytic Pt⁺-Mediated Oxidation of Methane by Molecular Oxygen in the Gas Phase**

Ralf Wesendrup, Detlef Schröder, and Helmut Schwarz*

Dedicated to Professor Heinz-Georg Wagner on the occasion of his 65th birthday

The activation of methane represents a fundamental challenge in chemistry, and the catalytic conversion of methane to methanol or formaldehyde is both of scientific and economic interest.^[1] At metal surfaces activation of methane often commences with a homolytic C–H bond cleavage and proceeds by reactions of the so-formed methyl radicals with an oxidant. Alternately, the reaction of methane with a transition metal center [M] may lead either to a metal-bonded hydrido methyl fragment, H–M–CH₃, or a carbene species, M=CH₂, with subsequent O-atom transfer to form the oxygenated products. Furthermore, direct oxidation of methane can be achieved by reactive oxo species, for example, high-valent transition metal oxides, which are recovered in the catalytic process. In a more classical fashion, methane functionalization may also proceed by ionic mechanisms in which either a proton or a hydride is abstracted or protonation take place.^[2]

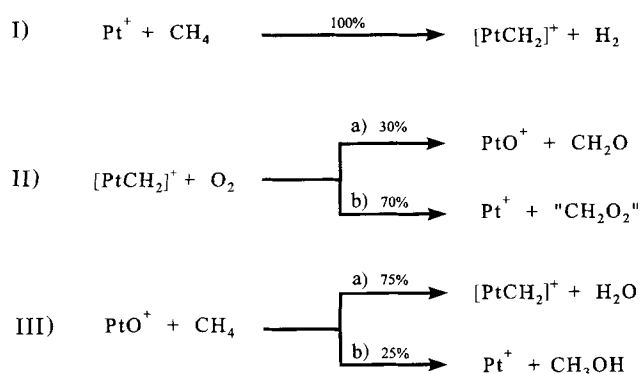
The high catalytic activity of platinum has been known since the last century, and platinum-based catalysts are widely used in reduction as well oxidation processes.^[3] Although heterogeneous catalysis is one of the most actively pursued research areas, this approach often fails to provide an understanding of the chemistry at a molecular level. In contrast, more direct mechanistic information may be obtained in gas-phase experiments in which the reactions of “naked” metal ions with neutral substrates can be probed under relatively well-defined conditions.^[4]

Recently, Irikura and Beauchamp^[1b, 5] discovered that “naked” third-row transition metal cations are capable of dehydrogenating methane in a stoichiometric fashion in the gas phase to yield the methylene complexes [M=CH₂]⁺.^[6] Here, we report the design and realization of a catalytic cycle^[7] for the gas-phase oxidation of methane under the conditions of Fourier transform ion cyclotron resonance (FT-ICR) mass spectrometry.^[8]

*] Prof. Dr. H. Schwarz, Dr. D. Schröder, R. Wesendrup
Institut für Organische Chemie der Technischen Universität
Strasse des 17. Juni 135, D-10623 Berlin (FRG)
Telefax: Int. code + (30)314-21102

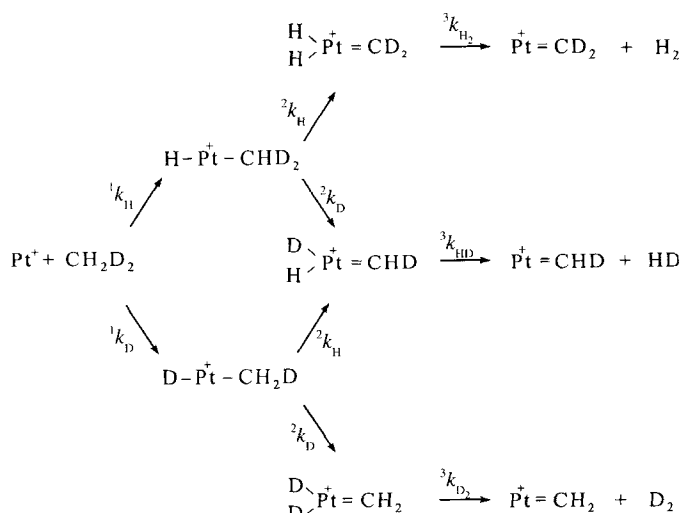
**] This work was supported by the Deutsche Forschungsgemeinschaft and the Fonds der Chemischen Industrie. We are grateful to Spectrospin AG, Fällanden, for the loan of a glow-discharge ion source, and Degussa AG, Hanau, for the generous supply of platinum targets.

As reported earlier,^[5] thermalized Pt⁺ ions dehydrogenate methane to yield the carbene complex [PtCH₂]⁺ (Scheme 1, process I). Although the rate constant k_R ($k_R = 8.2 \times 10^{-10} \text{ cm}^3 \text{ molecule}^{-1} \text{ s}^{-1}$) is somewhat smaller than the collision rate constant k_{ADO} ($k_{\text{ADO}} = 9.8 \times 10^{-10} \text{ cm}^3 \text{ molecule}^{-1} \text{ s}^{-1}$; ADO = average dipole orientation),^[9] the reaction is quite efficient if one takes into account that CH₄ is a small, symmetric molecule with low polarizability and strong C–H bonds. Thermochemical considerations^[10] lead to the conclusion that, since reaction I occurs at thermal energies, the reaction enthalpy (ΔH_f) for methane dehydrogenation is negative, and, thus, the heat of formation (ΔH_f) of [PtCH₂]⁺ is smaller than 316 kcal mol⁻¹; furthermore, the observation of reaction II (see below) sets a lower limit for $\Delta H_f[\text{PtCH}_2]^+$ at 308 kcal mol⁻¹; in the following, we will use an averaged value of $\Delta H_f[\text{PtCH}_2]^+ = 312 \pm 4 \text{ kcal mol}^{-1}$; from this one derives a Pt⁺–CH₂ bond dissociation energy of $\text{BDE}(\text{Pt}^+ - \text{CH}_2) = 115 \pm 4 \text{ kcal mol}^{-1}$.^[10b]



Scheme 1. Formation and reactions of [PtCH₂]⁺ and [PtO]⁺, as well as the formation of the methane oxidation products CH₃OH, CH₂O, and “CH₂O₂”.

The intramolecular kinetic isotope effects (KIEs) associated with the Pt⁺-mediated dehydrogenation of CH₂D₂ can be deduced from the relative abundance of [PtCD₂]⁺, [PtCHD]⁺, and [PtCH₂]⁺, which are formed in a 2.5:6.5:1.0 ratio. Because formation of [PtCHD]⁺ from CH₂D₂ is favored by a factor of 4 over the other two isotopomers, the statistically weighted ratio is 2.5:1.6:1.0 for H₂, HD, and D₂ losses, respectively. According to the mechanism depicted in Scheme 2, these data can be



Scheme 2. Scheme for the kinetics of the reactions of Pt⁺ and CH₂D₂.